

This is the peer reviewed version of the following article: F. Fanelli (corresponding author), S. Lovascio, R. d'Agostino, F. Arefi-Khonsari, F. Fracassi, Ar/HMDSO/O₂ fed Atmospheric Pressure DBDs: Thin film deposition and GC-MS investigation of by-products, Plasma Processes and Polymers 2010, 7, 535–543, which has been published in final form at <https://doi.org/10.1002/ppap.200900159>. This article may be used for non-commercial purposes in accordance with Wiley Terms and Conditions for Use of Self-Archived Versions. This article may not be enhanced, enriched or otherwise transformed into a derivative work, without express permission from Wiley or by statutory rights under applicable legislation. Copyright notices must not be removed, obscured or modified. The article must be linked to Wiley's version of record on Wiley Online Library and any embedding, framing or otherwise making available the article or pages thereof by third parties from platforms, services and websites other than Wiley Online Library must be prohibited.

Full Paper

Ar/HMDSO/O₂ fed Atmospheric Pressure DBDs:

Thin Film Deposition and GC-MS investigation of by-products

Fiorenza Fanelli,* Sara Lovascio, Riccardo d'Agostino, Farzaneh Arefi-Khonsari, Francesco

Fracassi

F. Fanelli, S. Lovascio, R. d'Agostino, F. Fracassi

Dipartimento di Chimica, Università degli Studi di Bari–IMIP CNR, via Orabona 4, 70126
Bari, Italy

Fax: +39 0805443405; E-mail: fiorenzafanelli@chimica.uniba.it

F. Arefi-Khonsari

Laboratoire de Génie des Procédés Plasmas et Traitements de Surfaces, EA3492, Université
Pierre et Marie Curie ENSCP, 11 rue Pierre et Marie Curie, Paris 75005, France

Summary

The thin film deposition in DBDs fed with Ar/HMDSO/O₂ mixtures was studied by comparing the FT-IR spectra of the deposits with the GC-MS analyses of the exhaust gas. Under the experimental conditions investigated, oxygen addition does not enhance the activation of the monomer while it highly influences the chemical composition and structure of the deposited coating as well as the quali-quantitative distribution of by-products in the exhaust. Without oxygen addition a coating with high monomer structure retention is obtained and the exhaust contains several by-products, such as silanes, silanols and linear and cyclic siloxanes. The dimethylsiloxane unit seems to be the most important building block of oligomers. Oxygen addition to the feed is responsible for an intense reduction of the organic character of the coating as well as for a steep decrease, below the quantification limit, of the concentration of all by-products except silanols. Some evidences induce to claim that the silanol groups contained in the deposits are formed through heterogeneous (plasma-surface) reactions.

Introduction

In the last decades the interest for organosilicon and silica-like thin films has continuously increased for their potential utilization in many technological fields,^[1] such as microelectronics,^[2-5] packaging,^[6,7] scratch-resistant materials,^[8] corrosion protection,^[9-12] biomaterials.^[13] Plasma-enhanced chemical vapour deposition (PE-CVD) has turned out to be a very attractive preparation method for these films since it is compatible with most materials, also sensitive to temperature increase (e.g. plastics, natural and synthetic fabrics, etc.), it allows to control film thickness, conformity, chemical composition and properties, etc..

Low pressure PE-CVD from organosilicon precursors is a well established technology since many papers and patents have been published so far,^[1-10, 13-26] unfortunately the high cost of vacuum equipments and the difficult integration in continuous production lines do not allow a wide utilization of this approach in large area manufacturing. In order to overcome these difficulties, many academic and industrial research groups are studying the PE-CVD from organosilicon and other precursors in non-equilibrium plasma at atmospheric pressure.^[27]

Among the various experimental ways to generate non equilibrium plasmas at atmospheric pressure, dielectric barrier discharge (DBD) technology is one of the most popular approach for thin film deposition and in particular for the production of SiO_x coatings (see for instance refs. 11-12 and 28-43) The critical point of the DBD technology is that uniform discharges (glow or Townsend regime^[44]) are difficult to obtain since in most cases inhomogeneous filamentary discharges are generated^[45]). Homogeneous discharges, similar to those obtained at low pressure, exist only in a narrow range of working parameters i.e. gas mixture composition, precursor concentration, frequency, applied voltage, etc.. Generally DBDs tend to be filamentary and hence intrinsically inhomogeneous, they can consequently produce non uniform and damaged coatings.^[29, 30, 36, 37] For instance it has been reported that with

N₂/HMDSO/N₂O mixtures the Townsend regime can be successfully obtained at HMDSO concentrations lower than few tens of ppm (e.g. 40 ppm^[33]) and that a stable homogeneous discharge can be generated at a maximum concentration of oxygen in nitrogen of 400 ppm.^[46] In order to obtain uniform and pinhole-free coatings in DBDs fed with organosilicon precursors the following approaches are reported: i) the deposition in a homogeneous regime;^[28, 32-34, 38, 39] ii) the optimization of filamentary discharges.^[29, 35, 41, 43]

Due to its non-toxic character, chemical inertness, and relatively high vapour pressure even at room temperature, hexamethyldisiloxane (HMDSO) is one of the most widely used “monomers” for the deposition of organosilicon and silica-like thin films both in low and atmospheric pressure plasmas. HMDSO reactivity in low pressure RF plasma has been investigated with many diagnostic techniques, such as Fourier transform infrared absorption spectroscopy (FT-IRAS), optical emission spectroscopy (OES), mass spectrometry (MS).^[7, 15, 16, 18, 20, 22-26] It was reported that the main electron impact dissociation path of HMDSO consists in a methyl loss and Si-O bond breaking.^[15, 16, 18] The oxygen addition to the gas mixture promotes homogeneous and heterogeneous oxidation producing partially oxidized fragments that can contribute to the film growth.^[7, 15, 16, 18] The diagnostic studies allowed to outline an overall deposition mechanism and to successfully correlate the plasma chemistry of HMDSO/O₂-containing low pressure plasmas with the chemical structure and final properties of the deposited coatings. Organic silicone-like coatings and inorganic SiO₂-like thin films can be in fact deposited by simply changing the oxygen content in the feed.^[7, 25]

Another diagnostic tool, useful to increase the knowledge on the deposition mechanism, is the analysis of exhaust gases by means of gas chromatography with mass spectrometry detection (GC-MS). Although an indirect analytical technique, not compatible with on-line and continuous sampling, GC-MS is a powerful tool which allows the evaluation of the precursor reactivity, the identification and eventually the quantification of the most abundant stable by-

products generated by plasma activation. Besides the pioneering work of Wróbel and co-workers,^[1, 17] who widely used this technique for studying thin film deposition in low pressure remote plasma fed with siloxanes and silanes, few authors have reported on this technique. Among them Sarmadi et al.^[14] and Fracassi et al.^[21] investigated the exhaust gases of low pressure RF plasma fed with HMDSO/O₂. Light hydrocarbons^[14] were detected along with different organosilicon compounds, most of them contained one or more dimethylsiloxane (-Me₂SiO-) groups,^[21] confirming the importance of this unit as building block in film growth.

Interesting results have also been published for atmospheric pressure cold plasmas containing HMDSO with the aim of correlating the plasma chemistry with the chemical composition and structure of the coating. Vinogradov et al.^[40, 41] performed the FT-IRAS and OES analysis of DBDs fed with Ar/HMDSO/O₂ and He/HMDSO/O₂. In particular the investigation of the plasma phase with FT-IRAS suggested that monomer fragmentation mainly results in the production of four radicals: (CH₃)₃SiO, Si(CH₃)₃, (CH₃)₃SiOSi(CH₃)₂ and CH₃; these reactive fragments can be responsible for the formation of pentamethyldisiloxane, trimethylsilane and methane. The concentration of these species decreases with oxygen addition, with the production of CO, CO₂, H₂CO, O₃ and HCOOH.

Also GC-MS was utilized to investigate organosilicon-containing atmospheric pressure plasmas. Sonnenfeld et al.^[31] studied HMDSO- and TEOS-fed filamentary discharges sustained in Ar, N₂ and He. It was reported that, in HMDSO-plasma, methyl loss with formation of pentamethyldisiloxane is the main reaction path in monomer activation along with Si-O bond breaking and formation of (CH₃)₃SiO and (CH₃)₃Si units. Since only small amounts of unidentified oligomers were detected, the authors assumed that the polymerization processes mainly take place at the surface of the growing polymer.

The present work reports a detailed GC-MS investigation of the exhaust of DBDs fed with Ar/HMDSO/O₂ gas mixtures. In particular the evolution of the most important species detected in the exhaust gas as a function of the oxygen-to-monomer feed ratio are compared with the FT-IR features of the deposits. The results allow to draw some important conclusions on the monomer activation, on the effect of the oxygen content in the feed and on the silanol groups formation in the deposit.

Experimental

Plasma processes were carried out in the home-made DBD reactor schematically shown in **Figure 1**. The discharge cell, enclosed in an airtight Plexiglas chamber (volume of about 14 L), consists of two 50x50 mm² parallel plate electrodes both covered by a 2.54 mm thick 70x70 mm² Al₂O₃ plate (CoorsTek, 96% purity). The interelectrode distance, that can be regulated with spacers, is fixed at 2 mm. The electrodes are connected to an AC HV (high voltage) power supply (SG2 STT Calvatron), composed of a corona generator and a HV transformer, working in the 15 – 50 kHz frequency range. Discharges were driven at fixed excitation frequency and voltage of 30 kHz and 2.5 kV_{rms}, respectively. The applied voltage (V) was measured by a HV probe (Tektronix P6015A); the current (I) and the charge (Q) were evaluated by measuring with a Tektronix P2200 probe the voltage drop across a 50 Ω resistor and a 4.7 nF capacitor connected in series with the grounded electrode, respectively. The data were recorded by means of a digital oscilloscope (Tektronix TDS2014B). The power dissipated in the discharge was evaluated employing the Manley method and in particular the voltage-charge (V-Q) Lissajous figure [45]. The dissipated power was expressed as specific power per unit of electrode surface.

Ar/HMDSO/O₂ mixtures were longitudinally injected in the discharge gap through a gas inlet slit and pumped out, by means of a membrane pump, through a slit placed at the opposite side of the gap. Gas flow canalization along the electrode length was assured by two glass spacers which laterally confine the interelectrode gap. The pressure in the chamber, measured by a MKS baratron, was kept constant at 760 Torr by pumping speed regulation with a needle valve.

Ar and O₂ (Air Liquide Argon C and Oxygen C) gas flow rates were controlled by MKS electronic mass flow controllers; HMDSO (Fluka, 98.5 % purity) vapours were introduced by an Ar stream bubbling through a liquid HMDSO reservoir kept at 30°C. The effective amount of precursor admitted into the reactor was evaluated by reservoir weight variation per unit time and, assuming an ideal gas behaviour, it was converted to flow rate expressed in sccm.

Experiments were performed by keeping constant the Ar and HMDSO flow rates at 4000 sccm and 1 sccm respectively, and changing the O₂ flow rate in order to vary the O₂-to-HMDSO feed ratio in the range 0 – 40. Under these conditions the gas residence time in the interelectrode zone was equal to about 80 ms.

Before each experiment, the Plexiglas chamber was purged with 4000 sccm of Ar for 20 min to remove air contaminations. The deposition processes were carried out for 5 min.

The deposition rate was evaluated by measuring the films thickness by an Alpha-Step 500 KLA Tencor Surface Profilometer on partially masked thin glass slides placed on the bottom ground electrode. Measurements were performed at different position along the gas flow, i.e. at different gas residence times; for each experimental condition the mean value in the region between 20 and 30 mm from the gas entrance inside the discharge area was considered.^[47]

The bulk chemical characterization of the coatings was performed by Fourier transform infrared spectroscopy (FT-IR). Films deposited onto 1 cm², 0.7 mm thick c-Si(100) substrates were analyzed with a commercial Bruker Equinox 554 FTIR Interferometer in the 400-4000 cm⁻¹ range, with a resolution of 4 cm⁻¹. To minimize water vapour and carbon dioxide

interferences the spectrometer optical path was purged with a continuous N₂ flow for 10 min between each measurement. The analyses were performed on samples positioned on the alumina plate that covers the ground electrode both inside the discharge zone (20 - 30 mm from the gas entrance) and downstream of the electrode area (50 - 60 mm from the gas entrance) (Figure 1).

In order to collect stable by-products formed by plasma activation, the exhaust gas was sampled for 30 min with a stainless steel liquid nitrogen trap located between the reactor and the pump (Figure 1). After sampling, the trap was isolated from the system, the condensate was dissolved in acetone (Sigma-Aldrich, 99.8 % purity) and the solution was filtered and analyzed by means of a GC 8000^{Top} gaschromatographer (Thermoquest Corporation) coupled with a differential pumped quadrupole mass spectrometer (Voyager, Thermoquest Corporation). A Grace ATTM-1MS fused silica capillary column (polydimethylsiloxane 0.25 μm thick stationary phase, length of 30 m, internal diameter of 0.25 mm) was utilized with He as carrier gas (2 sccm) under the following conditions: injector temperature of 200°C, column temperature programmed from 30°C to 200°C (1 min at 30°C, linear heating rate of 10°C·min⁻¹, 1 min at 200°C). Separated products were analyzed at the GC-MS interface and mass spectrometer source temperature of 250 and 200°C, respectively. Mass spectra were recorded in full-scan mode in the *m/z* range 15–500 amu at the standard ionizing electron energy of 70 eV. Stable by-products were identified by means of available libraries,^[48] some species were tentatively identified through the interpretation of their mass spectra according to the typical fragmentations pattern of organosilicon compounds. The identification of some products was confirmed by the comparison of retention time and mass spectrum with standard compounds. Nonane (Aldrich, 99% purity) was used as internal standard (IS) for quantitative analysis of identified species; calibration curves were calculated in the linear range utilizing the area of the corresponding peaks in the chromatogram acquired in total ion current. The measured amounts have then been converted in flow rate. The extent of reacted HMDSO,

namely the HMDSO depletion percentage ($\text{HMDSO}_{\text{depletion}}$), was evaluated according to equation (1):

$$\text{HMDSO}_{\text{depletion}} (\%) = \frac{\text{HMDSO}_{\text{off}} (\text{sccm}) - \text{HMDSO}_{\text{on}} (\text{sccm})}{\text{HMDSO}_{\text{off}} (\text{sccm})} \cdot 100 \quad (1)$$

where $\text{HMDSO}_{\text{off}}$ and HMDSO_{on} are the precursor flow rates detected in the exhaust in plasma off and plasma on conditions, respectively. Considering the overall procedure utilized (sampling, GC-MS analysis conditions, etc.) the limit of quantification (LOQ) of by-products in the exhaust was 0.0001 sccm.

Results and discussion

Under the experimental conditions explored in this work a filamentary DBD was obtained. In fact, as appears in **Figure 2**, the current signals at various O_2/HMDSO feed ratios show several peaks characteristic of filamentary discharges.^[45] The filamentary character seems to increase with the oxygen content in the feed gas since the number of current peaks increases within each half-cycle. In particular at a O_2 -to-HMDSO feed ratio of 0 the discharge current is formed by a quasi-periodical multipeak signal and the filamentary discharge is characterized by a quasi-homogeneous appearance ascribed to stochastically distributed microdischarges; under this condition only few filaments (defined in ref. 49 as a family of streamers which repeatedly generate in the same spot) were observed in the gas gap. At a O_2 -to-HMDSO ratio of 25 the typical current signal of a filamentary DBD characterized by intense and well-distinguished filaments is observed.

With increasing the O_2 -to-HMDSO feed ratio from 0 to 25 the average specific discharge power increased from 0.20 to 0.33 $\text{W} \cdot \text{cm}^{-2}$.

Transparent and compact coatings without appreciable powder formation were deposited with Ar/HMDSO/O₂ feeds, while without oxygen an oily film was obtained. Powder deposition occurred downstream of the electrode region especially at high O₂/HMDSO ratios. Since powder formation in the discharge zone has been reported for DBD fed with O₂ and HMDSO,^[30, 38] it is reasonable to assume that under our experimental conditions, due to the high flow rate (i.e. low residence time) the gas phase reactions responsible of powder formation occur outside the discharge zone and/or that the processes responsible of powder formation and deposition are scarcely efficient in the plasma zone. The latter possibility is supported by the work of Borra^[50] where it is reported that the deposition of charged nanoparticles is prevented in parallel plate DBDs driven at a frequency higher than 10 kHz (our DBD is driven at 30 kHz), due to poor collection efficiency.

The deposition rate varies in the 120-150 nm·min⁻¹ range, and it is not significantly affected by O₂ content. On the contrary the films chemistry is markedly affected by oxygen addition. In **Figure 3** the normalized FT-IR spectra of coatings deposited at O₂-to-HMDSO ratios 0 and 25 are shown (Figures 3a and 3c). For both conditions also the FT-IR spectra of the deposit collected on a silicon substrate positioned downstream of the electrode region are reported for comparison (Figures 3b and 3d).

The film deposited inside the discharge region without oxygen (Figure 3a) shows the typical features of silicone-like films: the intense Si-O-Si asymmetric stretching band at 1042 cm⁻¹, the Si-(CH₃)_x symmetric bending at 1258 cm⁻¹, and the CH_x absorptions in the 2850 – 3000 cm⁻¹ region (i.e. intense CH₃ asymmetric stretching at 2959 cm⁻¹, weak CH₃ symmetric stretching at 2874 cm⁻¹, and CH₂ asymmetric stretching at 2900 cm⁻¹).^[1, 2, 4, 5, 7, 19, 24, 25] The absorptions in the 750 - 900 cm⁻¹ region suggest the presence of di- and tri-substituted Si-(CH₃)_x moieties.^[1, 2, 4, 5, 7, 19, 24, 25] The intense peak at 841 cm⁻¹ can be assigned to the Si-C rocking in Si-(CH₃)₃; the strong absorption at 796 cm⁻¹ (which also contains a contribution due to Si-O-Si bending reported in literature at 800 cm⁻¹) is due to Si-C rocking in Si-(CH₃)₂.

The significant presence of Si-(CH₃)₂, i.e. chain-propagating units, and Si-(CH₃)₃, i.e. chain-terminating units, is further confirmed by the position of Si-(CH₃)_x absorption at 1258 cm⁻¹. It has been reported, in fact, that the position of Si-(CH₃)_x signal shifts at lower wavenumbers as the number of methyl groups bonded to silicon increases.^[2, 4, 5] The absorptions due to mono-substituted Si-CH₃, di-substituted Si-(CH₃)₂ and tri-substituted Si-(CH₃)₃ are in fact generally observed at about 1275 cm⁻¹, 1260 cm⁻¹ and 1255 cm⁻¹,^[2, 4, 5] respectively. The fact that in this work the Si-(CH₃)_x band was found at 1258 cm⁻¹ suggests the deposition of poorly crosslinked coating with high monomer structure retention, in fact oily films are obtained.

The film also contains some Si-H units as confirmed by the presence of the Si-H stretching at 2124 cm⁻¹^[1, 2, 4, 5, 7, 19, 24] and, since the typical OH absorption in the 3200-3600 cm⁻¹ region is not evident, the small shoulder at 907 cm⁻¹ can be attributed to H-Si-O hybrid vibrations^[2] and not to Si-OH bending.^[1, 7, 19, 25]

As expected, in the FT-IR spectra of coatings deposited inside the discharge zone at O₂-to-HMDSO ratio of 25, a marked reduction of absorptions due to carbon containing groups (i.e. CH_x and Si(CH₃)_x) is observed (Figure 3c). The CH₃ asymmetric stretching at 2970 cm⁻¹ shifts to higher wavenumbers for the more oxidized chemical environment and the Si-(CH₃)_x absorption at 1274 cm⁻¹ suggests the prevalence of mono-substituted Si-CH₃ units and therefore a higher crosslinking of the deposited coating. This is also confirmed by the reduced absorptions of Si-C rocking in Si-(CH₃)₃ at 841 cm⁻¹ and Si-(CH₃)₂ at 800 cm⁻¹. The broad OH absorption appears in the 3200 – 3600 cm⁻¹ region and, since any Si-H can be detected, the intense signal at 905 cm⁻¹ can be ascribed to silanol (Si-OH) groups. The intense Si-O-Si asymmetric stretching slightly moves to higher wavenumbers, 1050 cm⁻¹, with a shoulder around 1123 cm⁻¹ likely due to short Si-O-Si chains.^[2, 4, 5] The position of Si-O-Si asymmetric stretching is in agreement with the presence of carbon containing groups since in SiO₂-like coating this absorption falls at 1070 cm⁻¹ and shift at lower wavenumbers as the carbon

content increases.^[4, 7, 19] Thus it can be concluded that, under our experimental conditions, also at high O₂-to-HMDSO feed ratio an appreciable amount of residual carbon is still present in the deposit even though the reduced IR absorption of carbon-containing groups and the predominance of mono-substituted Si-CH₃ units suggests the formation of more oxidized and crosslinked coatings.

Figures 3b and 3d show the FT-IR spectra of the downstream deposits. Without oxygen addition, no significant differences with respect to the film deposited inside the discharge zone can be detected, while at O₂-to-HMDSO ratio of 25 (Figure 3d), the deposit consists of powders and higher absorptions of CH_x and Si-(CH₃)_x groups are evident as compared to the film deposited inside the discharge zone. Also a different shape of Si-O-Si asymmetric stretching can be appreciated due to the marked increase of the shoulder at 1123 cm⁻¹ that could be related to a less dense, less ordered network of the collected powders with respect to the coating deposited in the discharge zone.^[4, 5]

FT-IR spectra allow making some considerations on the HMDSO deposition mechanism in DBDs. In agreement with published data,^[7, 11, 14, 19, 24, 25, 30, 40, 41] without oxygen addition the deposit is mainly polydimethylsiloxane-like with HMDSO structure retention; thus, as also confirmed by FT-IR spectra, (CH₃)₃Si-O-Si(CH₃)₂, Si-(CH₃)₃, Si(CH₃)_xO (x = 2, 3) units could be considered representative of the main film precursors chemical structure. At high oxygen content in the feed a partial oxidation of these reactive fragments occurs. The lower organic character of the film deposited inside the discharge region with respect to the powders collected downstream of the electrode region suggests that part of the oxidation reactions in the discharge zone occurs on the surface of the growing film. A quite similar carbon content should be expected both for the film deposited in the discharge zone and for the downstream powder without heterogeneous oxidation in the discharge zone.

The GC-MS investigation of by-products showed that under all the experimental condition explored the amount of reacted HMDSO ($\text{HMDSO}_{\text{depletion}}$) was always higher than 50 %. As reported in **Figure 4**, oxygen addition to the gas feed does not improve monomer activation/utilization since HMDSO depletion is always lower than without oxygen. Moreover the increase of the specific power observed as a function of the oxygen content in the feed does not result in an increase of the monomer utilization.

The decrease of the monomer depletion with oxygen addition could be due to the variation of the discharge electrical regime. As shown in Figure 2, oxygen addition increases the filamentary character of the discharge, i.e. the plasma is less homogeneous and more concentrated in the filaments and, therefore, the effective plasma volume, wherein electron impact and most chemical reactions occur, is smaller. As a consequence, the overall monomer activation is less efficient.

On the other hand, the decrease of HMDSO utilization as a function of the oxygen addition could be also due to the fact that oxygen molecules or atoms are not responsible of the HMDSO activation (i.e. the first step of the overall reaction mechanism). The main monomer activation channel could be electron impact, as it was already reported for HMDSO in RF low pressure plasmas^[21] even though other authors observed different trends.^[23, 25] Another possibility is that the activation of HMDSO is due to Ar metastables which are also responsible of oxygen activation and therefore, when the O_2 content of the feed increases, the monomer activation is reduced because Ar metastables are mainly involved in oxygen activation with a consequent decrease of the monomer depletion.

A list of the identified by-products detected in the exhaust gas is reported in **Table 1**. There are silanes with low molecular mass, (i.e. trimethylsilane, tetramethylsilane ethyltrimethylsilane), silanols (i.e. trimethylsilanol and hydroxypentamethyldisiloxane) as well as linear and cyclic compounds with up to 5 silicon atoms and general formula $\text{Me}-(\text{Me}_2\text{SiO})_n-\text{SiMe}_3$ ($n = 1-4$) and $(\text{Me}_2\text{SiO})_n$ ($n = 3-4$), respectively, which derive from

oligomerization processes: i.e. chain propagation and ring formation or expansion. In agreement with FT-IR analyses of deposited films, species containing one or two Si-H bonds and CH₂ moieties (e.g. ethylpentamethyldisiloxanes) were found. These species could form for the recombination of the active species formed by plasma activation; these recombination reactions could occur either in the plasma phase or outside the discharge zone and could involve both ionic and neutral species (such as radicals) leading to the stable products retained by the cold trap. If the sampling procedure employed in this study is considered, it seems reasonable to assume that heavier compounds (e.g. compounds containing more than five Si atoms) are not sampled for their low volatility, while light species (e.g., CO, CO₂, CH₄, SiH₄, etc.) are lost during manipulation of the condensate for their high volatility. As reported in **Figure 5**, disiloxanes (i.e. pentamethyldisiloxane, tetramethyldisiloxane, ethylpentamethyldisiloxane) concentration steeply decreases with oxygen addition to the feed gas; among them pentamethyldisiloxane is the most abundant by-product.

Similar results are shown in **Figure 6** for methyltrisiloxanes. All concentrations decrease below the quantification limit increasing the O₂ content in the feed. Moreover it was observed that the trisiloxane concentration in the exhaust is higher as the number of methyl groups in the molecule increases (i.e. octamethyltrisiloxane > 1,1,1,3,5,5,5-heptamethyltrisiloxane > 1,1,3,3,5,5-hexamethyltrisiloxane).

It seems that oligomerization proceeds mainly through condensation of precursors with a chemical structure close to that of HMDSO (e.g. pentamethyldisiloxanyl units); some dangling bond left after methyl loss are saturated by Si-H bonds formation. The reduction of oligomerization with oxygen addition is realistically due to the oxidation of oligomerizing species.

Also the amount of silanols, i.e. trimethylsilanol and hydroxypentamethyldisiloxane, decreases with oxygen addition to the feed (**Figure 7**) but, unlike the other species, they can be quantified also at high O₂ addition since they are never below the quantification limit of

the analytical procedure. The trends of silanols in the gas phase depend on the fact that oxygen promotes both the formation of Si-OH units and the oxidation of organic fragments to form CO₂ and H₂O.

If the trend of Figure 7 is compared to the FT-IR spectra of Figure 3c and 3d, which show higher amounts of Si-OH in the deposits collected inside the discharge and downstream at high O₂/HMDSO ratio, when the silanols content in the exhaust is very low, it can be concluded that the formation of the Si-OH groups present in the coatings occurs mainly on the film surface through heterogeneous reactions during the growth process. Without oxygen addition to the feed, although the quantity of silanols in the exhaust is maximum (Figure 7), no absorption of Si-OH groups can be detected in the FT-IR spectra of deposits collected both in the discharge zone and downstream (Figure 3a and 3b). This evidence allows to enhance the hypothesis that silanols formed in the plasma phase, even at high concentrations, are not incorporated in the growing coating. Silanols are formed on the film surface during the deposition for reaction with oxygen.

Without oxygen addition to the feed, apart from the unreacted monomer, pentamethyldisiloxane, (CH₃)₃Si-O-Si(CH₃)₂H, and hydroxypentamethyldisiloxane, (CH₃)₃Si-O-Si(CH₃)₂OH, are the most abundant species in the exhaust. Both compounds could be formed from one HMDSO molecule with the substitution of a methyl group (with -H and -OH, respectively) indicating that under the experimental conditions utilized, Si-CH₃ bond breaking surely plays an important role in HMDSO activation and film growth.^[31, 41]

Conclusions

In this work, thin film deposition in DBDs fed with Ar/HMDSO/O₂ gas mixtures was studied by comparing the FT-IR spectra of the deposits with the GC-MS analyses of the exhaust.

Without oxygen addition the coating is characterized by a predominant organic character, as the starting monomer. Several by-products, such as silanes, silanols and linear and cyclic siloxanes, are detected in the exhaust. The dissociation of the Si-CH₃ bond in the monomer molecule plays an important role in monomer activation, even through the Si-O bond scission can not be neglected as evidenced by the presence of silanes in the exhaust. Both FT-IR spectra and GC-MS analyses show that the (CH₃)₃Si-O-Si(CH₃)₂, Si-(CH₃)₃ and Si(CH₃)_xO (x = 2, 3) units could be representative of the chemical structure of the film and of the by-products; in particular the dimethylsiloxane (-Si(CH₃)₂O-) repeating unit can be considered to be the most important building block in the oligomerization. As also found in some cases in low pressure plasmas, oxygen addition to the feed gas does not improve monomer activation since the HMDSO depletion does not increase by adding oxygen to the feed. The effect of oxygen addition to monomer depletion could be due to the fact that the discharge is more filamentary and a smaller plasma volume is available for HMDSO activation. Nevertheless oxygen strongly influences the chemical characteristics of the deposits and the composition of the exhaust. As expected, the concentration of all organic by-products, except silanols, is reduced below the quantification limit as a function of the oxygen content in the feed. Some evidences induce to claim that the silanols contained in the deposits are formed through heterogeneous (plasma-surface) reaction during film growth and not from the contribution of silanol-containing species formed in the plasma.

Acknowledgements: The authors gratefully acknowledge the *Regione Puglia* financial support (CIP: PE_083).

Keywords: dielectric barrier discharges (DBD), FT-IR, gaschromatography-mass spectrometry (GC-MS), hexamethyldisiloxane (HMDSO), plasma-enhanced chemical vapour deposition (PE-CVD)

References

- [1] A. M. Wróbel, M. Wertheimer, *Plasma Deposition, Treatment, and Etching of Polymers*, R. d'Agostino ed., Academic Press, New York 1990, p. 163.
- [2] A. Grill, *J. Appl. Phys.* **2003**, *93*, 1785.
- [3] M. Creatore, W. M. M. Kessels, Y. Barrell, J. Benedikt, M. C. M. van de Sanden, *Mat. Sci. Semicond. Process.* **2004**, *7*, 283.
- [4] A. Milella, J. L. Delattre, F. Palumbo, F. Fracassi, R. d'Agostino, *J. Electrochem. Soc.* **2006**, *153*, F106.
- [5] A. Milella, F. Palumbo, J. L. Delattre, F. Fracassi, R. d'Agostino, *Plasma Process. Polym.* **2007**, *4*, 425.
- [6] M. Creatore, F. Palumbo, R. d'Agostino, P. Fayet, *Surf. Coat. Technol.* **2001**, *142-144*, 163.
- [7] M. Creatore, F. Palumbo, R. d'Agostino, *Plasmas Polym.* **2002**, *7*, 291.
- [8] L. Zajičková, V. Buršíková, J. Janča, *Vacuum* **1998**, *50*, 19.
- [9] L. Zajičková, V. Buršíková, V. Peřina, A. Macková, D. Subedi, J. Janča, S. Smirnov, *Surf. Coat. Technol.* **2001**, *142-144*, 449.
- [10] F. Fracassi, R. d'Agostino, F. Palumbo, E. Angelini, S. Grassini, F. Rosalbino, *Surf. Coat. Technol.* **2003**, *174*, 107.
- [11] C. Petit-Etienne, M. Tatoulian, I. Mabile, E. Sutter, F. Arefi-Khonsari, *Plasma Process. Polym.* **2007**, *4*, S562.
- [12] J. Bour, J. Bardon, H. Aubriet, D. Del Frari, B. Verheyde, R. Dams, D. Vangeneugden, D. Ruch, *Plasma Process. Polym.* **2008**, *5*, 788.
- [13] T. Hayakawa, M. Yoshinari, K. Nemoto, *Biomaterials* **2004**, *25*, 119.

- [14] A. M. Sarmadi, T. H. Ying, F. Denes, *Eur. Polym. J.* **1995**, *31*, 847.
- [15] M. R. Alexander, F. R. Jones, R. D. Short, *Plasmas Polym.* **1997**, *2*, 277.
- [16] M. R. Alexander, F. R. Jones, R. D. Short, *J. Phys. Chem. B* **1997**, *101*, 3164.
- [17] A. M. Wrobel, A. Walkiewicz-Pietrzykowska, S. Wickramanayaka, Y. Hatanaka, *J. Electrochem. Soc.* **1998**, *145*, 2866.
- [18] D. Magni, Ch. Deschenaux, Ch. Hollenstein, A. Creatore, P. Fayet, *J. Phys. D: Appl. Phys.* **2001**, *34*, 87.
- [19] G. Borvon, A. Goulet, A. Granier, G. Turban, *Plasmas Polym.* **2002**, *7*, 241.
- [20] D. Theirich, Ch. Soll, F. Leu, J. Engemann, *Vacuum* **2003**, *71*, 349.
- [21] F. Fracassi, R. d'Agostino, F. Fanelli, A. Fornelli, F. Palumbo, *Plasmas Polym.* **2003**, *8*, 259.
- [22] M. Goujon, T. Belmonte, G. Henrion, *Surf. Coat. Technol.* **2004**, *188-189*, 756.
- [23] K. Li, O. Gabriel, J. Meichsner, *J. Phys. D: Appl. Phys.* **2004**, *37*, 588.
- [24] P. Raynaud, B. Despax, Y. Segui, H. Caquineau, *Plasma Process. Polym.* **2005**, *2*, 45.
- [25] D. S. Wavhal, J. Zhang, M. L. Steen, E. R. Fisher, *Plasma Process. Polym.* **2006**, *3*, 276.
- [26] S. Saloum, M. Naddaf, B. Alkhaled, *Vacuum* **2008**, *82*, 742.
- [27] S. E. Alexandrov, M. L. Hitchman, *Chem. Vap. Dep.* **2005**, *11*, 457.
- [28] Y. Sawada, S. Ogawa, M. Kogoma, *J. Phys. D: Appl. Phys.* **1995**, *28*, 1661.
- [29] R. Thyen, A. Weber, C.-P. Klages, *Surf. Coat. Technol.* **1997**, *97*, 426.
- [30] K. Schmidt-Szalowski, Z. Rżanek-Boroch, J. Sentek, Z. Rymuza, Z. Kusznierevicz, M. Misiak, *Plasmas Polym.* **2000**, *5*, 173.
- [31] A. Sonnenfeld, T. M. Tun, L. Zajičková, K. V. Kozlov, H. E. Wagner, J. F. Behnke, R. Hippler, *Plasmas Polym.* **2001**, *6*, 237.
- [32] F. Massines, N. Gherardi, A. Fornelli, S. Martin, *Surf. Coat. Technol.* **2005**, *200*, 1855.
- [33] I. Enache, H. Caquineau, N. Gherardi, T. Paulmier, L. Maechler, F. Massines, *Plasma Process. Polym.* **2007**, *4*, 806.

- [34] N. Gherardi, L. Maechler, C. Sarra-Bournet, N. Naudé, F. Massines, *ISPC19*, Bochum, 2009.
- [35] X. Zhu, F. Arefi-Khonsari, C. Petit-Etienne, M. Tatoulian, *Plasma Process. Polym.* **2005**, 2, 407.
- [36] R. Maurau, D. Duday, H.-N. Migeon, J. Amouroux, F. Arefi-Khonsari, *ISPC18*, Kyoto, 2007.
- [37] R. Maurau, A. Dembele, N. D. Boscher, D. Duday, P. Choquet, F. Arefi-Khonsari, *ISPC19*, Bochum, 2009.
- [38] S. Starostine, E. Aldea, H. de Vries, M. Creatore, M. C. M. van de Sanden, *Plasma Process. Polym.* **2007**, 4, S440.
- [39] S. Starostine, A. Premkumar, M. Creatore, H. de Vries, R. Paffen, M. van de Sanden, *ISPC19*, Bochum, 2009.
- [40] I. Vinogradov, D. Zimmer, A. Lunk, *Plasma Process. Polym.* **2007**, 4, S435.
- [41] I. Vinogradov, D. Zimmer, A. Lunk, *Plasma Process. Polym.* **2009**, 6, DOI: 10.1002/ppap.200931102.
- [42] B. Twomey, M. Rahman, G. Byrne, A. Hynes, L.-A O'Hare, L. O'Neill, D. Dowling, *Plasma Process. Polym.* **2008**, 5, 737.
- [43] R. Morent, N. De Geyter, S. Van Vlierberghe, P. Dubruel, C. Leys, E. Schacht, *Surf. Coat. Technol.* **2009**, 203, 1366.
- [44] F. Massines, P. Segur, N. Gherardi, C. Khamphan, A. Ricard, *Surf. Coat. Technol.* **2003**, 174-175, 8.
- [45] U. Koghelschatz, *Plasma Chem. Plasma Process.* **2003**, 23, 1.
- [46] F. Massines, G. Gouda, N. Gherardi, M. Duran, E. Croquesel, *Plasmas Polym.* **2001**, 6, 35.
- [47] F. Fanelli, F. Fracassi, R. d'Agostino, *Plasma Process. Polym.* **2005**, 2, 688.

[48] NIST and Wiley libraries in *MassLab Release 1.4 (GC/MS Data System Software Finnigan)*.

[49] *"Plasma chemistry"*, A. Fridman, Cambridge University Press, New York 2008.

[50] J.-P. Borra, *J. Phys. D: Appl. Phys.* **2006**, *39*, R19.

Figure captions

Figure 1. Schematic of the experimental apparatus

Figure 2. Current and voltage waveforms of the DBD fed with Ar/HMDSO/O₂ gas mixtures, at different O₂/HMDSO feed ratios: a) 0, b) 1; c) 25.

Figure 3. FT-IR spectra of plasma-polymerized coatings and relative deposits obtained inside the discharge zone and downstream of the electrode region at O₂/HMDSO ratios 0 and 25 a) discharge zone at O₂/HMDSO = 0; b) downstream at O₂/HMDSO feed ratio = 0; c) discharge zone at O₂/HMDSO = 25; d) downstream at O₂/HMDSO = 25.

Figure 4. Reacted HMDSO (HMDSO_{depletion}) trend in the exhaust as a function of the O₂/HMDSO ratio in the feed.

Figure 5. Tetramethylsiloxane, pentamethylsiloxane, and ethylpentamethylsiloxane flow rate in the exhaust gas as a function of the O₂/HMDSO ratio in the feed.

Figure 6. Octamethyltrisiloxane, 1,1,1,3,5,5,5-heptamethyltrisiloxane and 1,1,3,3,5,5-hexamethyltrisiloxane flow rate in the exhaust gas as a function of the O₂/HMDSO ratio in the feed.

Figure 7. Trimethylsilanol and hydroxypentamethyldisiloxane flow rate in the exhaust gas as a function of the O₂/HMDSO ratio in the feed.

Table 1. Identified species detected in the exhaust gas of Ar/HMDSO/O₂ fed DBD

	Compound	Formula
1	Trimethylsilane	Si(CH ₃) ₃ H
2	Tetramethylsilane	Si(CH ₃) ₄
3	Ethyltrimethylsilane	Si(C ₂ H ₅)(CH ₃) ₃
4	Trimethylsilanol	Si(CH ₃) ₃ OH
5	1,1,3,3-Tetramethyldisiloxane	(CH ₃) ₂ HSi-O-Si(CH ₃) ₂ H
6	Pentamethyldisiloxane	(CH ₃) ₃ Si-O-Si(CH ₃) ₂ H
7	Hexamethyldisiloxane	(CH ₃) ₃ Si-O-Si(CH ₃) ₃
8	Ethylpentamethyldisiloxane	(CH ₃) ₃ Si-O-Si(C ₂ H ₅)(CH ₃) ₂
9	Hydroxypentamethyldisiloxane	(CH ₃) ₃ Si-O-Si(CH ₃) ₂ OH
10	1,1,3,3,5,5-Hexamethyltrisiloxane	H-(Si(CH ₃) ₂ O) ₂ -Si(CH ₃) ₂ H
11	Hexamethylcyclotrisiloxane	(Si(CH ₃) ₂ O) ₃
12	1,1,1,3,5,5,5-Heptamethyltrisiloxane	(CH ₃) ₃ Si-O-Si(CH ₃)H-O-Si(CH ₃) ₃
13	1,1,1,3,3,5,5-Heptamethyltrisiloxane	CH ₃ -(Si(CH ₃) ₂ O) ₂ -Si(CH ₃) ₂ H
14	Octamethyltrisiloxane	CH ₃ -(Si(CH ₃) ₂ O) ₂ -Si(CH ₃) ₃
15	1-Ethyl-1,1,3,3,5,5,5-heptamethyltrisiloxane	C ₂ H ₅ -(Si(CH ₃) ₂ O) ₂ -Si(CH ₃) ₃
16	3-Ethyl-1,1,1,3,5,5,5-heptamethyltrisiloxane	(CH ₃) ₃ Si-O-Si(CH ₃)(C ₂ H ₅)-O-Si(CH ₃) ₂
17	Octamethylcyclotetrasiloxane	(Si(CH ₃) ₂ O) ₄
18	1,1,1,3,3,5,7,7,7-Nonamethyltetrasiloxane	CH ₃ -(Si(CH ₃) ₂ O) ₂ -Si(CH ₃)H-O-Si(CH ₃) ₃
19	1,1,1,3,3,5,5,7,7-Nonamethyltetrasiloxane	CH ₃ -[Si(CH ₃) ₂ O] ₃ -Si(CH ₃) ₂ H
20	Decamethyltetrasiloxane	CH ₃ -[Si(CH ₃) ₂ O] ₃ -Si(CH ₃) ₃
21	2,2,4,4,5,5,7,7-Octamethyl-3,6-dioxa-2,4,5,7-tetrasilaoctane	(CH ₃) ₃ Si-O-Si(CH ₃) ₂ -Si(CH ₃) ₂ -O-Si(CH ₃) ₃
22	Dodecamethylpentasiloxane	CH ₃ -[Si(CH ₃) ₂ O] ₄ -Si(CH ₃) ₃

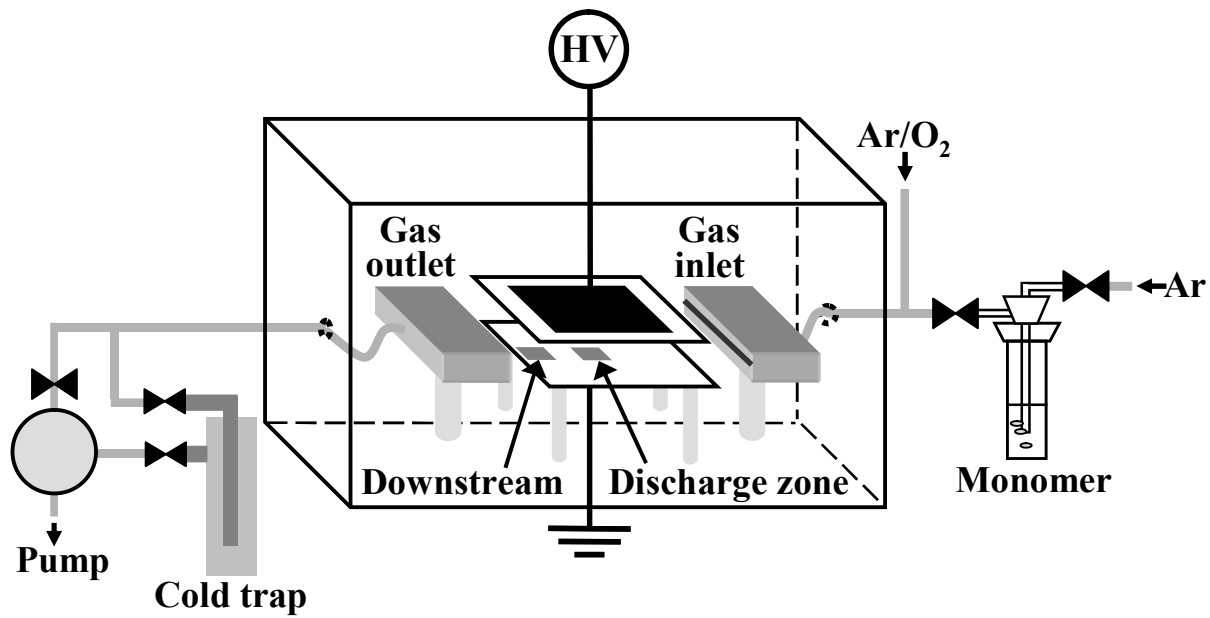


Figure 1. Schematic of the experimental apparatus

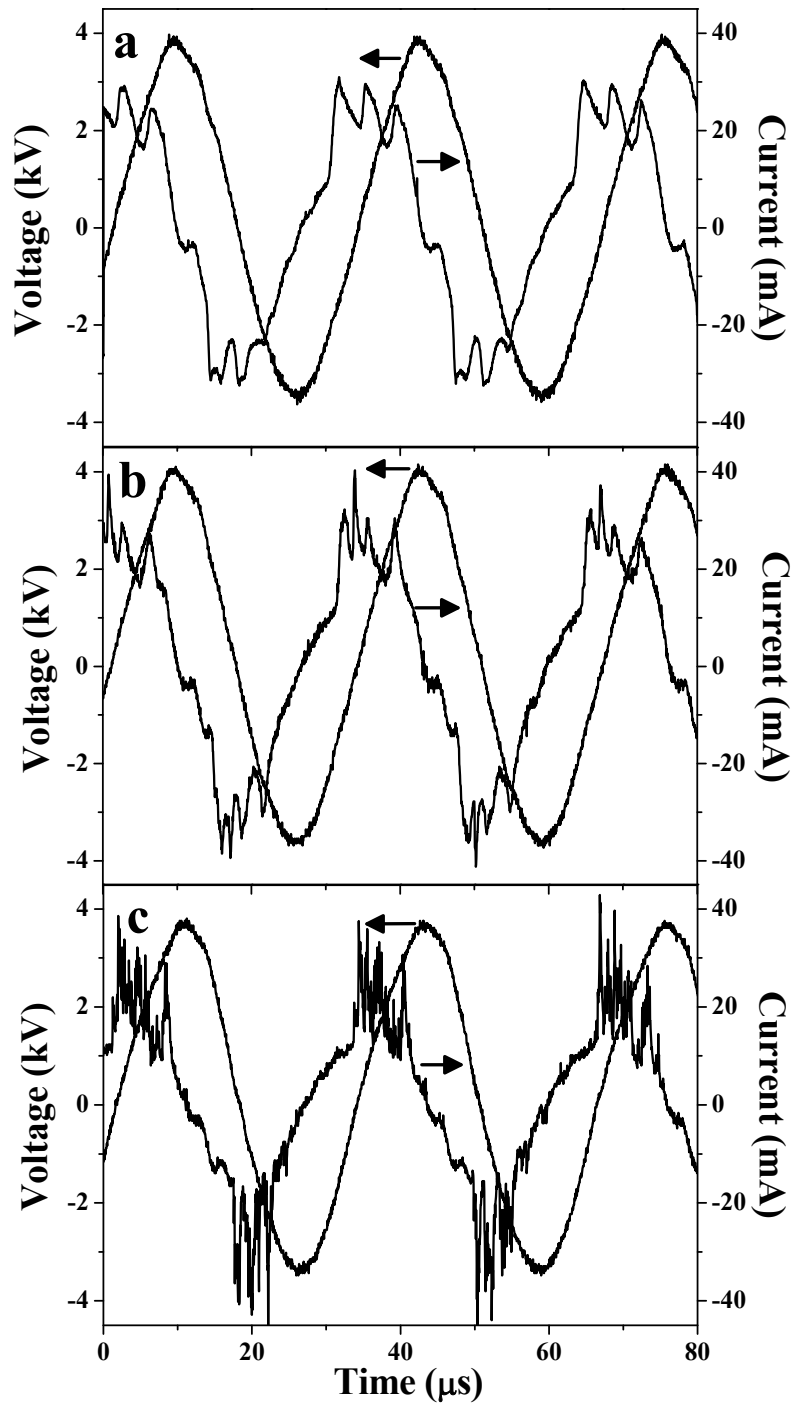


Figure 2. Current and voltage waveforms of the DBD fed with Ar/HMDSO/O₂ gas mixtures, at different O₂/HMDSO feed ratios: a) 0, b) 1; c) 25.

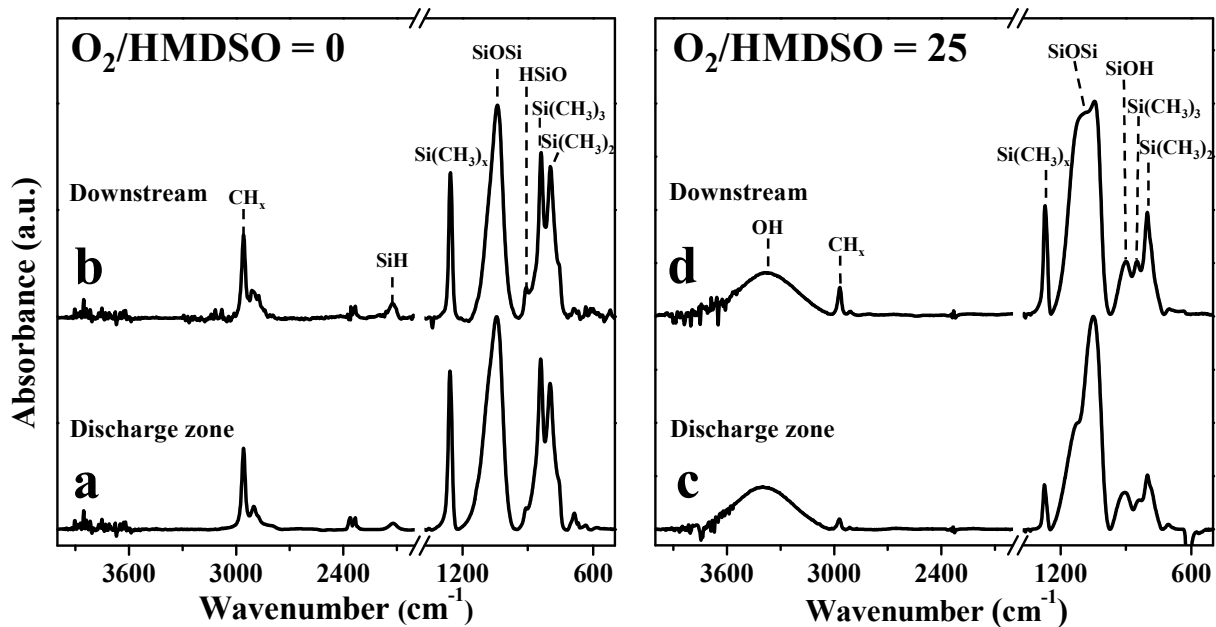


Figure 3. FT-IR spectra of plasma-polymerized coatings and relative deposits obtained inside the discharge zone and downstream of the electrode region at $O_2/HMDSO$ ratios 0 and 25 a) discharge zone at $O_2/HMDSO = 0$; b) downstream at $O_2/HMDSO$ feed ratio = 0; c) discharge zone at $O_2/HMDSO = 25$; d) downstream at $O_2/HMDSO = 25$.

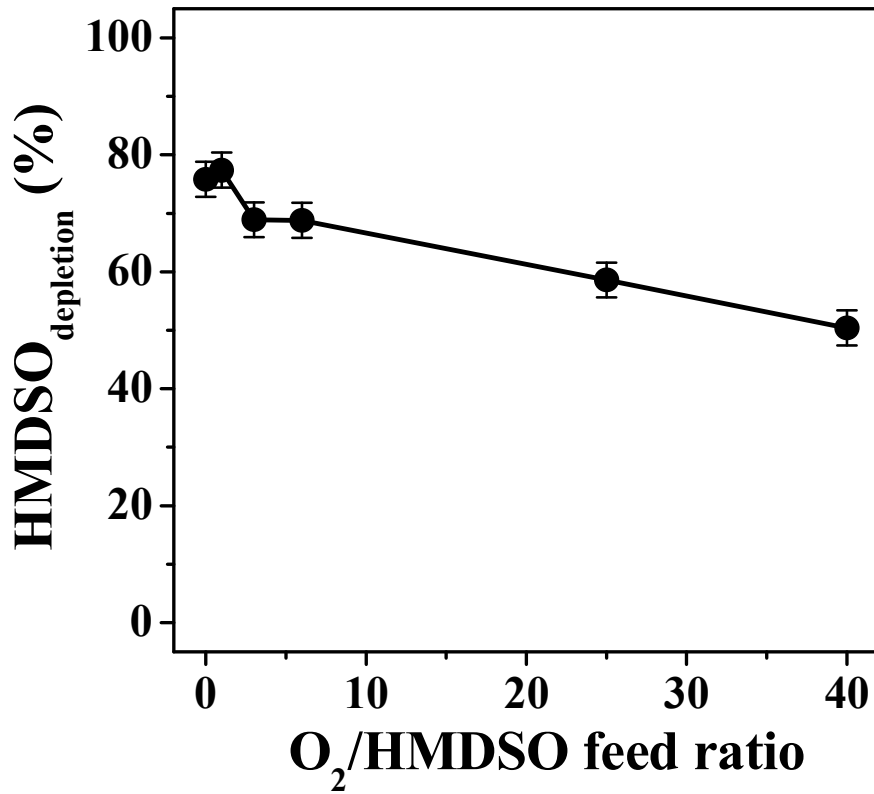


Figure 4. Reacted HMDSO (HMDSO_{depletion}) trend in the exhaust as a function of the O₂/HMDSO ratio in the feed.

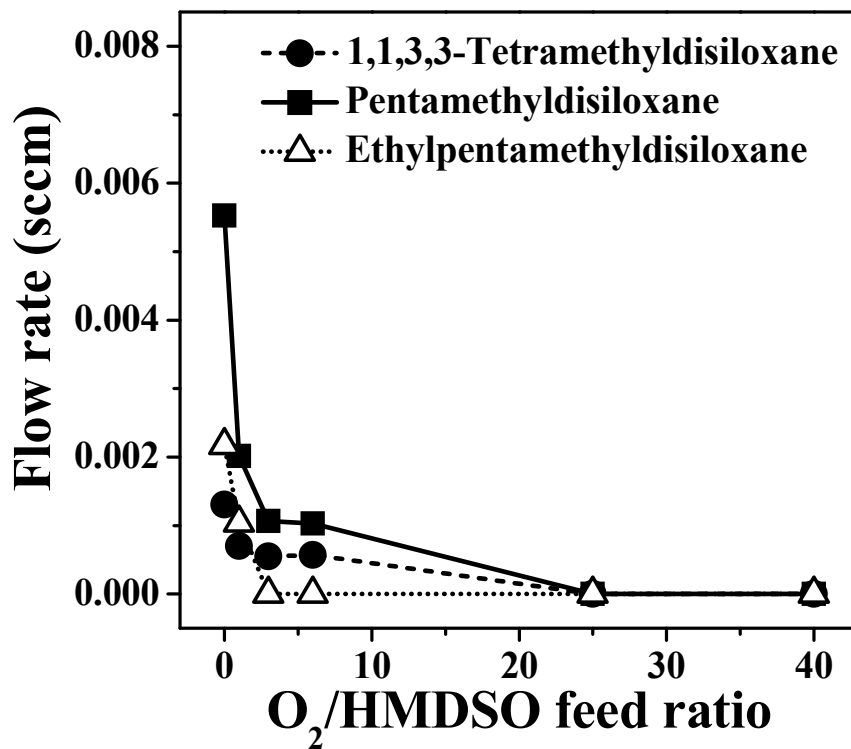


Figure 5. Tetramethyldisiloxane, pentamethyldisiloxane, and ethylpentamethyldisiloxane flow rate in the exhaust gas as a function of the O₂/HMDSO ratio in the feed.

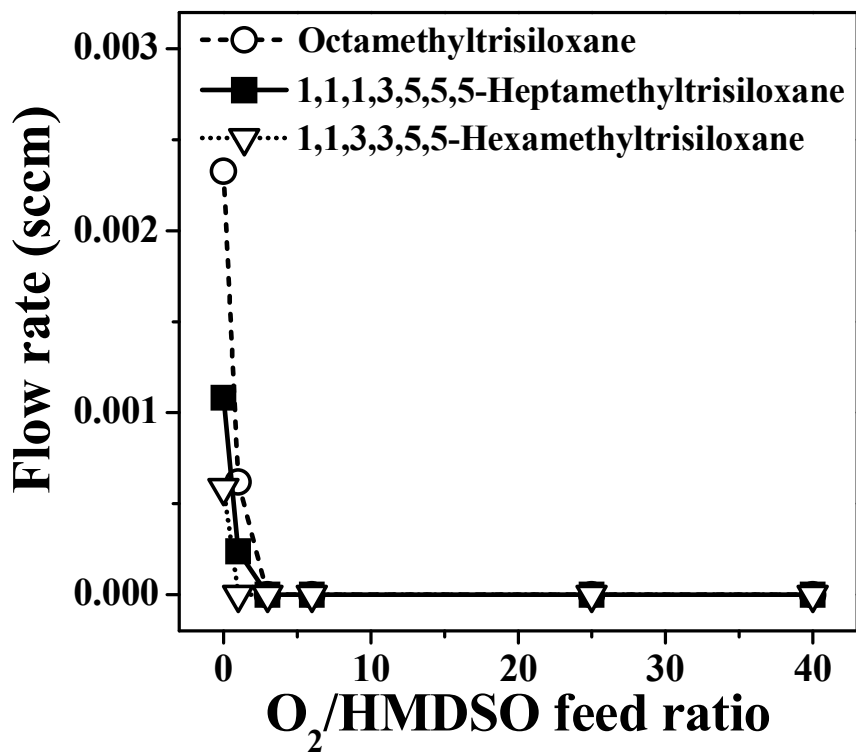


Figure 6. Octamethyltrisiloxane, 1,1,1,3,5,5,5-heptamethyltrisiloxane and 1,1,3,3,5,5-hexamethyltrisiloxane flow rate in the exhaust gas as a function of the O₂/HMDSO ratio in the feed.

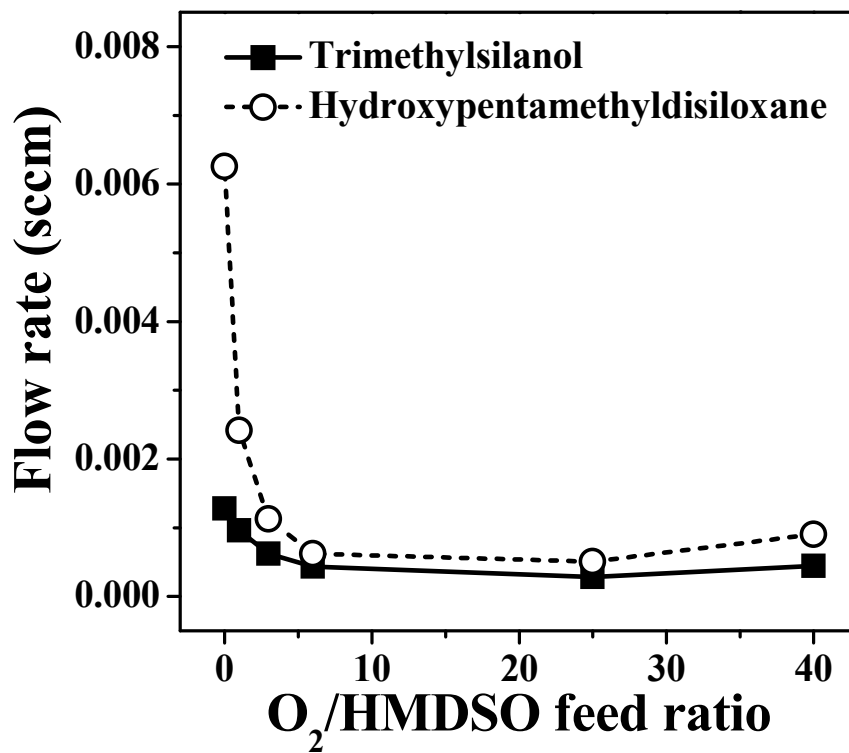


Figure 7. Trimethylsilanol and hydroxypentamethyldisiloxane flow rate in the exhaust gas as a function of the O₂/HMDSO ratio in the feed.

Text and Figure for the Table of Contents

Full Paper

In this work the PE-CVD of organosilicon coatings in Ar/HMDSO/O₂ fed atmospheric pressure DBDs is presented through a comparison between the GC-MS investigation of the exhaust gas and the FT-IR analyses of the deposits. Oxygen addition is responsible for a reduction of the organic character of the coatings and for a steep decrease, below the quantification limit, of all by-products except silanols (see Figure).

Fiorenza Fanelli,* Sara Lovascio, Riccardo d'Agostino, Farzaneh Arefi-Khonsari, Francesco Fracassi

Ar/HMDSO/O₂ fed Atmospheric Pressure DBDs: Thin Film Deposition and GC-MS investigation of by-products

